

Supporting Information

The Concentration Dependence of the Number of Rubrene Molecules around the NC

In 1 mL cyclohexane solution (the concentration of NC is $C_{NC}=8.14 \times 10^{-6}$ mol/L, and the concentration of rubrene is C_{RUB}), the number of rubrene molecules (N_{RUB}) within a range of r_i ($r_1=5$ nm, $r_2=10$ nm, $r_3=20$ nm) around a nanoparticle with a radius of 10 nm (R) can be expressed as follows:

$$N_{RUB} = 10^{-24} \times \frac{4}{3} \pi \times \left((r_i + R)^3 - R^3 \right) \times C_{RUB} \times N_A \quad (I)$$

where N_A is the Avogadro constant.

For sample 5, $C_{NC}=8.14 \times 10^{-6}$ mol/L, $C_{RUB}=1.0$ mg/mL= 1.875×10^{-3} mol/L. The number of rubrene molecules, according to eq. (I), within a range of 10 nm around a nanoparticle with a radius of 10 nm can be calculated as:

$$N_{RUB} = 10^{-24} \times \frac{4}{3} \pi \times \left((r_i + R)^3 - R^3 \right) \times C_{RUB} \times N_A = 33$$

The ratio (Z%) of rubrene molecules in the nanoparticle range of 10 nm to all rubrene molecules in solution is as follows:

$$Z\% = \frac{N_{RUB} \times V \times C_{NC} \times N_A}{V \times C_{RUB} \times N_A} = 14.1\% \quad (II)$$

where V is the volume of the solution mentioned above.

The Calculation of Lifetime

The lifetime values were calculated according the following equation: ¹

$$\tau_{\text{avg}} = \frac{\int_0^{\infty} tI(t)d_t}{\int_0^{\infty} I(t)d_t} \quad (\text{III})$$

where $I(t)$ is the emission intensity at time t .

The Förster distance (R_0)

In our model for calculation, we assume that in a 1 mL of sample solution each NC occupies an average volume of V . This space is approximated by a sphere with a radius ($r_{\text{max}}+R$), where r_{max} is the furthest distance between rubrene and the NC in the solution:

$$r_{\text{max}} = \sqrt[3]{\frac{3}{4\pi \times C_{\text{NC}} \times N_A}} - R \quad (\text{IV})$$

The distance (r) between the NC and rubrene molecule is:

$$r = \frac{\int_0^{r_{\text{max}}} \left(\frac{d_{N_{\text{RUB}}}}{d_{r_i}} \right) \bullet r_i d_i}{N_{\text{RUB}} \Big|_{r_i=r_{\text{max}}}} \quad (\text{V})$$

For the sample with rubrene concentration of 2.0 mg/mL, the energy transfer efficiency by the Förster-type process (by ${}^4\text{S}_{3/2} \rightarrow \text{S}_1$) is 4.08%. According to eq. (I), (II), (IV), (V) and (4) (main text), we find

$$R_0 = 10.5 \text{ nm}$$

$$Z\% = 16.0\%$$

For the sample with rubrene concentration of 0.25 mg/mL, the energy transfer efficiency by the Förster-type process (by ${}^4\text{S}_{3/2} \rightarrow \text{S}_1$) is 1.01%. According to eq. (I), (II), (IV), (V) and (4) (main text), we find

$$R_0 = 8.4 \text{ nm}$$

$$Z\% = 11.0\%$$

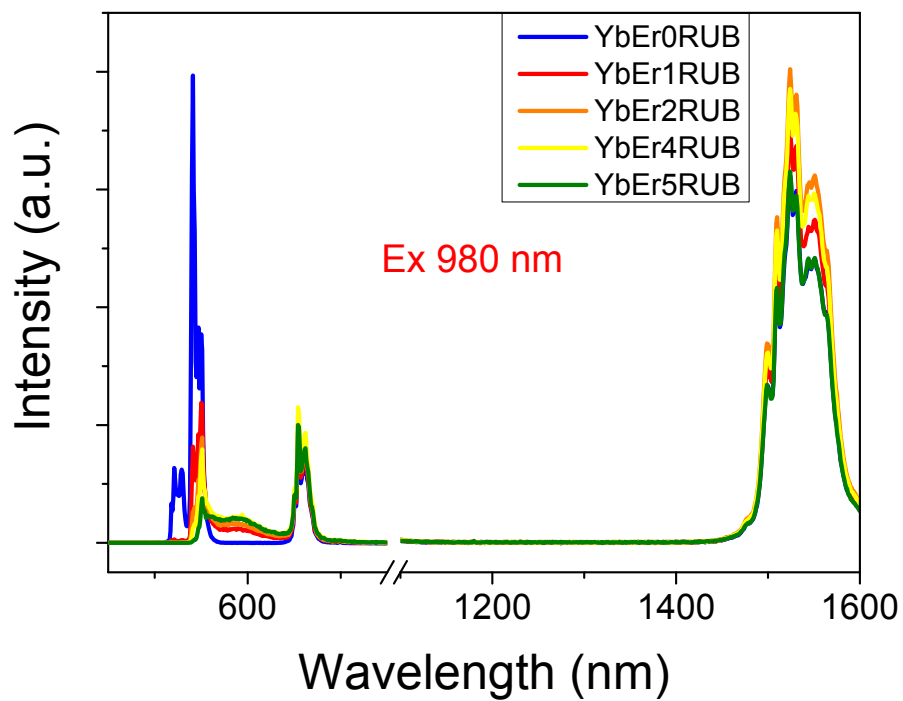
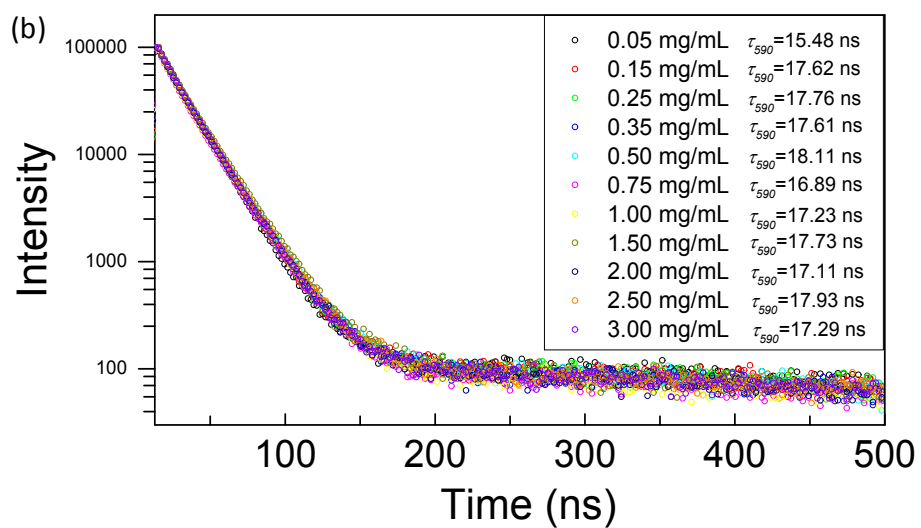
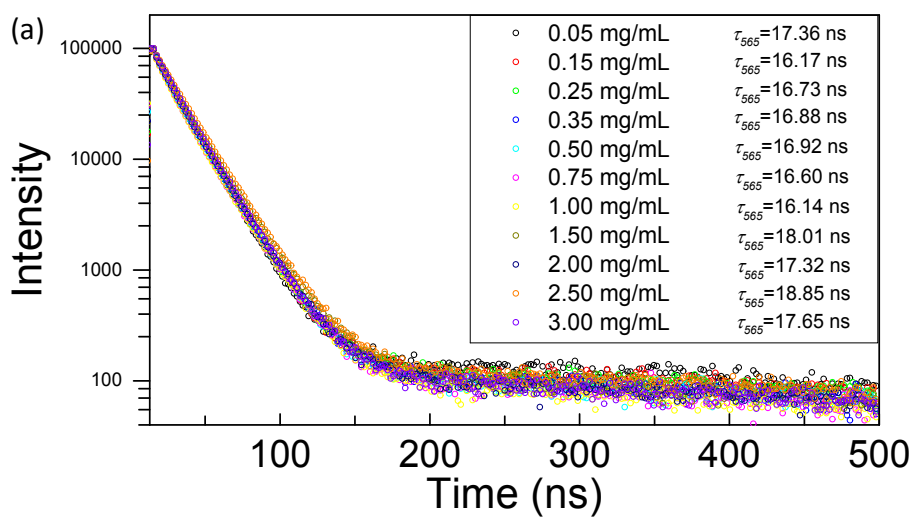


Fig. S1. Visible-infrared emission spectra of $\text{NaYF}_4:20\%\text{Yb}^{3+}/1\%\text{Er}^{3+}@\text{Rubrene}$ with varying concentrations of rubrene molecules under 980 nm excitation.



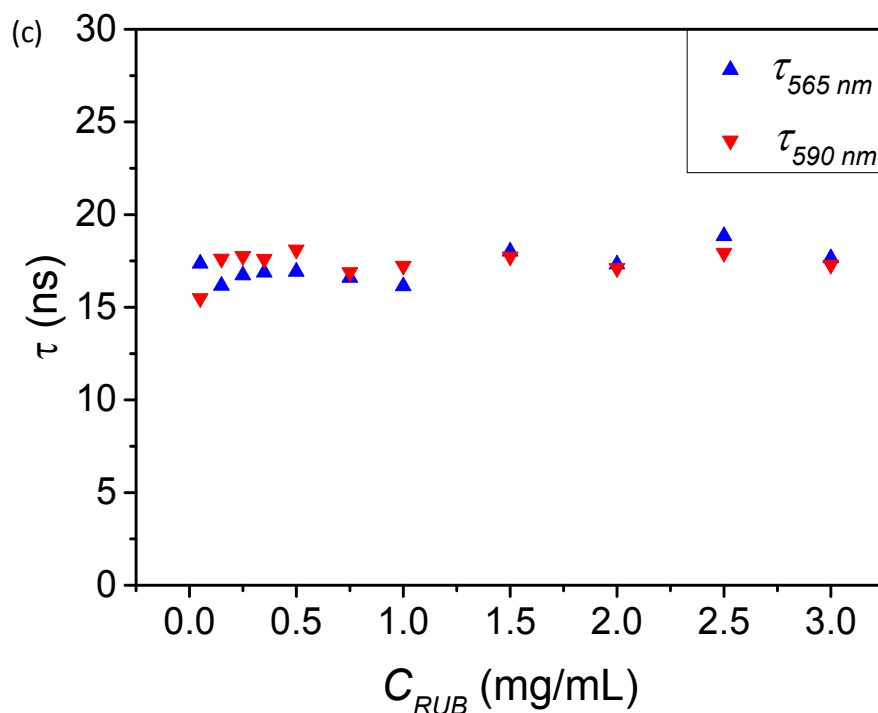


Fig. S2. (a, b) Prompt fluorescence decay curves of rubrene solution (without nanoparticles) with different concentrations recorded at 565 nm (a) and 590 nm (b). (c) Fluorescence lifetime versus concentration.

In Fig. 5 (main text), there are two peaks located at 565 nm and 590 nm in the fluorescence spectra of rubrene excited at 450 nm. It can be seen that the fluorescent spectrum of rubrene show a clear concentration dependence. As the rubrene concentration increases, the peak intensity ratio I_{565}/I_{590} decreases gradually. At low rubrene concentrations (0.05-0.25 mg/mL), the peak ratio of 565 nm to 590 nm is greater than 1, and when the concentration is higher (0.35-3.0 mg/mL), the peak ratio of 565 nm to 590 nm is less than 1. At the same time, with the increase of rubrene concentration, the intensity of both fluorescence peaks decreases (0.25-3.0 mg/mL) after the increase in the concentration range of 0.05-0.15 mg/mL. In addition, Fig. S2 (a)(b)(c) show that the increase in the rubrene concentration does not result in a significant change in the rubrene fluorescence lifetime, which imply that the concentration does not affect its fluorescence lifetime within the examined concentration range (0.05-3.0 mg/mL) of rubrene. The fluorescence concentration dependence of rubrene is caused by the self-absorption of rubrene. When the concentration is low (0.05-0.15 mg/mL), the fluorescence intensity increases with the increase of the rubrene concentration due to the increase number of density of chromophores. When the concentration is high (0.25-3.0 mg/mL), self-absorption becomes more and more significant, resulting in a decrease in the fluorescence intensity of rubrene. The absorption spectrum of rubrene solution shows that rubrene has absorption below 600 nm, and the rubrene self-absorption near 565 nm is higher than that near 590 nm. Therefore, the strong self-absorption leads to the concentration-dependent emission spectrum of rubrene. In addition,

the change in rubrene fluorescence peak shapes of samples containing different rubrene concentrations in Fig. S3 can be also explained by the self-absorption of rubrene.

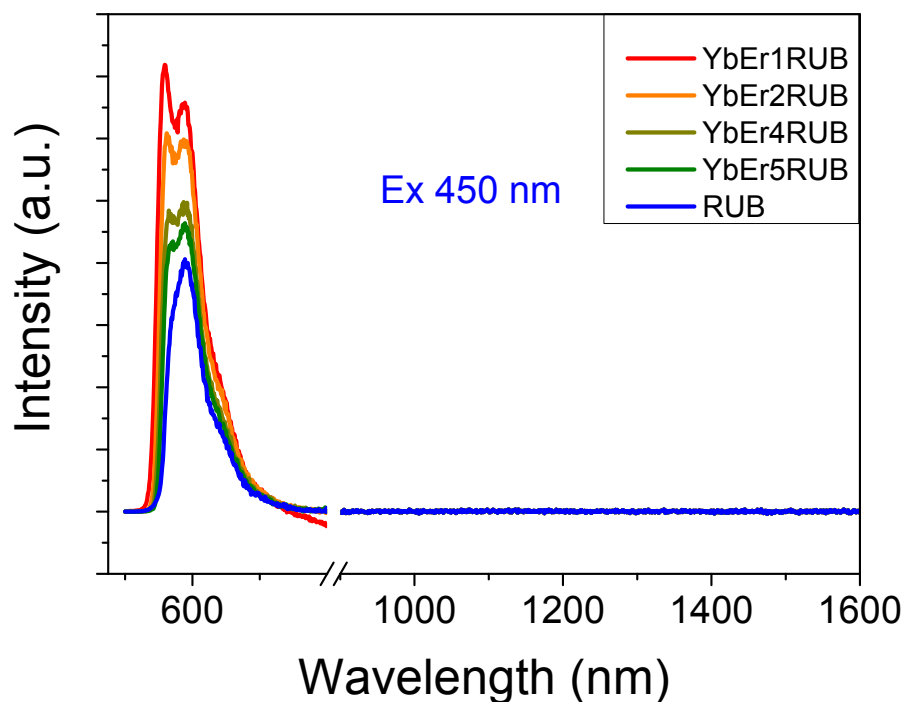


Fig. S3. Visible-infrared emission spectra of rubrene and $\text{NaYF}_4:20\% \text{Yb}^{3+}/1\% \text{Er}^{3+}@\text{Rubrene}$ with varying concentrations of rubrene molecules under 450 nm excitation.

In Fig. S3, only the emission from rubrene molecules is observed, indicating that energy transfer from rubrene to RE-doped nanoparticles does not occur. This can be explained by the smaller absorption cross-section of RE ions (Er^{3+}) at the visible spectral range. In addition, the variation in the emission spectra of rubrene can be rationalized by the self-absorption of rubrene, as we mentioned previously.

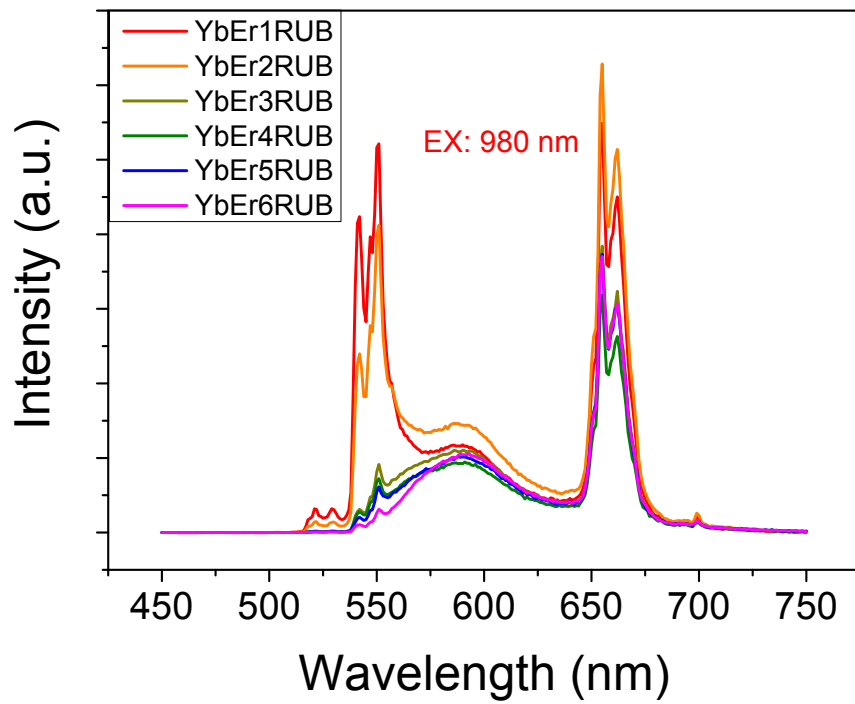


Fig. S4. Visible upconversion emission spectra of NaYF₄:20%Yb³⁺/1%Er³⁺@Rubrene with varying concentrations of rubrene molecules under 980 nm excitation. These spectra are plotted with the same set of data as Fig. 3d in the main text.

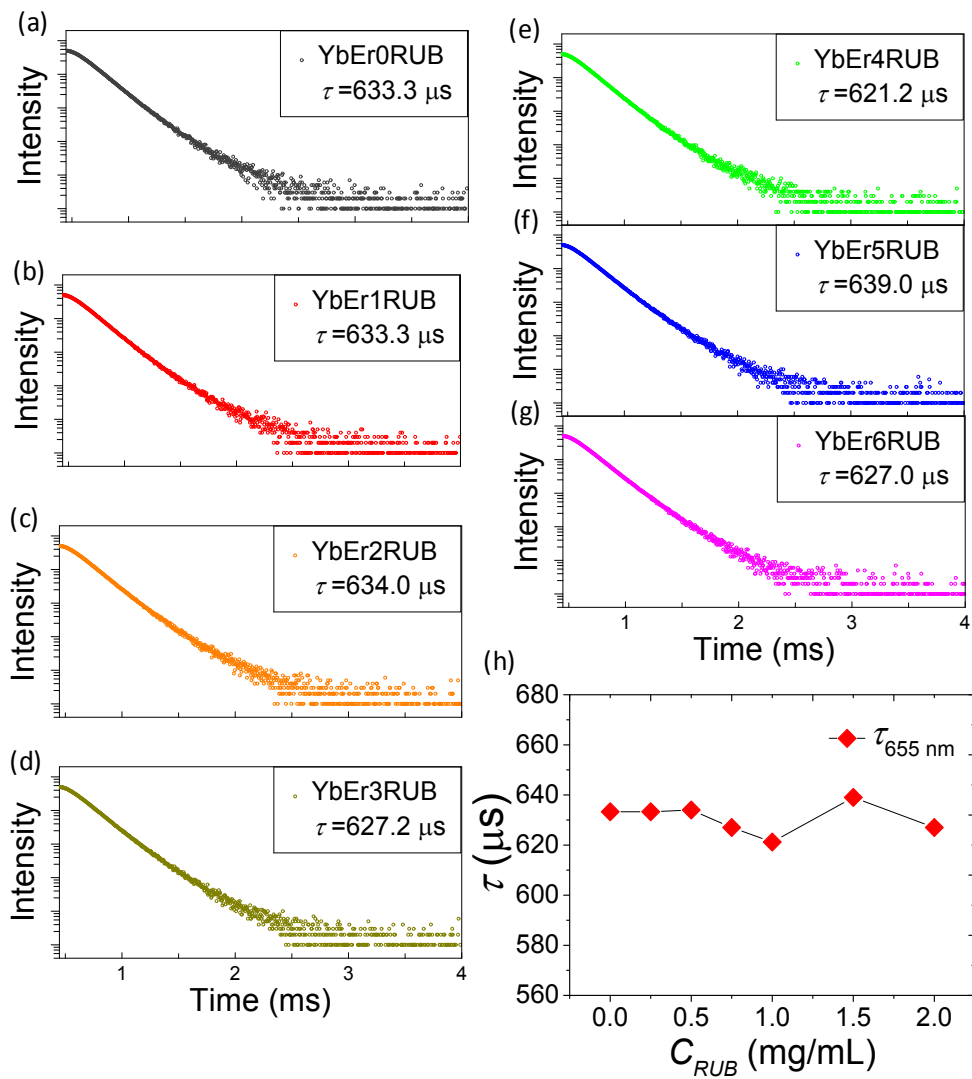


Fig. S5. (a)-(g) Prompt fluorescence decay curves of NaYF₄:20%Yb³⁺/1%Er³⁺@Rubrene in cyclohexane. The lifetime of sample was measured at 655 nm under 980 nm pulse laser excitation. (h) The lifetime versus concentration of rubrene (0-2.0 mg/mL).

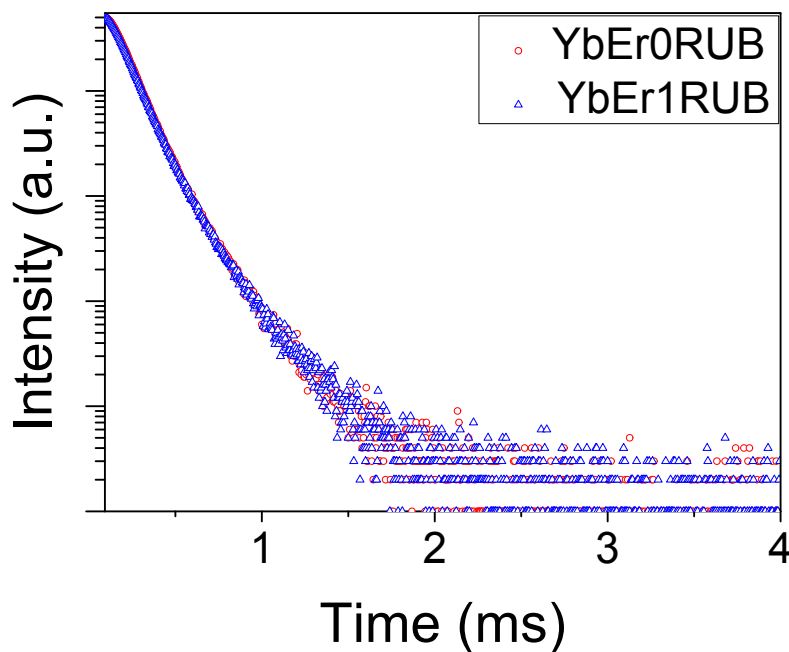


Fig. S6. Prompt emission decay curves at 522 nm of NaYF₄: 20%Yb³⁺/1%Er³⁺ NCs (sample 1) and NaYF₄: 20%Yb³⁺/1%Er³⁺ @Rubrene (sample 2) in cyclohexane.

Fig. S6 shows that there is almost no change in the fluorescence lifetime (522 nm of Er³⁺) of sample 2 compared to sample 1, suggesting that no resonance energy occurs between ²H_{11/2} of Er³⁺ and S₁ of rubrene in Sample 2 with a low rubrene concentration (0.25 mg/mL). According to eqs.(I),(V),(VI), the average distance between NC and rubrene in sample 2 is 55.9 nm. This distance is far beyond the range of resonance energy transfer and does not meet the conditions of resonance energy transfer, which is consistent with the results above. Therefore, the quenching of the Er³⁺ 522 nm can be only ascribed to re-absorption of emission by rubrene molecules.

As depicted in Fig. S4, for samples with higher rubrene concentration, the 522 nm emission peak of Er³⁺ disappears completely due to strong reabsorption of rubrene, making it difficult to measure its fluorescence lifetime. So we did not do the fluorescence lifetime of 522 nm for other samples.

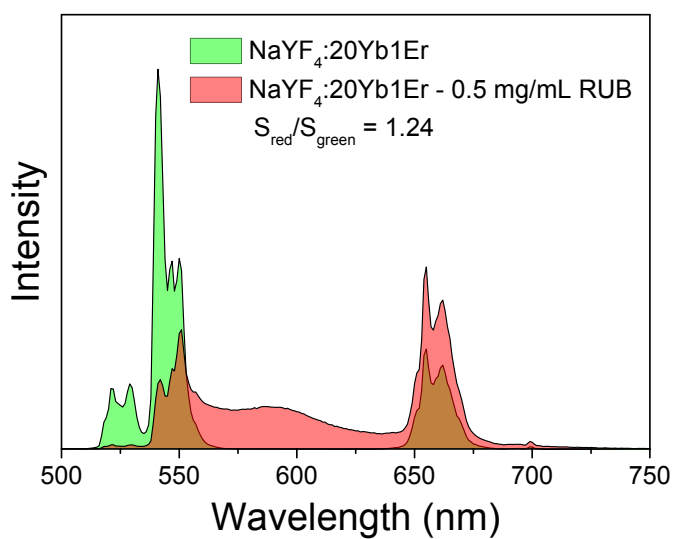


Fig. S7 Visible upconversion emission spectra of pure NaYF₄:20%Yb³⁺/1%Er³⁺ and hybrid system with 0.5 mg/mL Rubrene under 980 nm excitation.

Table S1. The changes of spectral intensity (in total)

Sample	Sample 2	Sample 3	Sample 4	Sample 5	Sample 6	Sample 7
C_{RUB} (mg/mL)	0.25	0.50	0.75	1.0	1.5	2.0
$I_{NCS-RUB}/I_{pure\ NCS}$	1.19	1.24	0.71	0.60	0.65	0.63

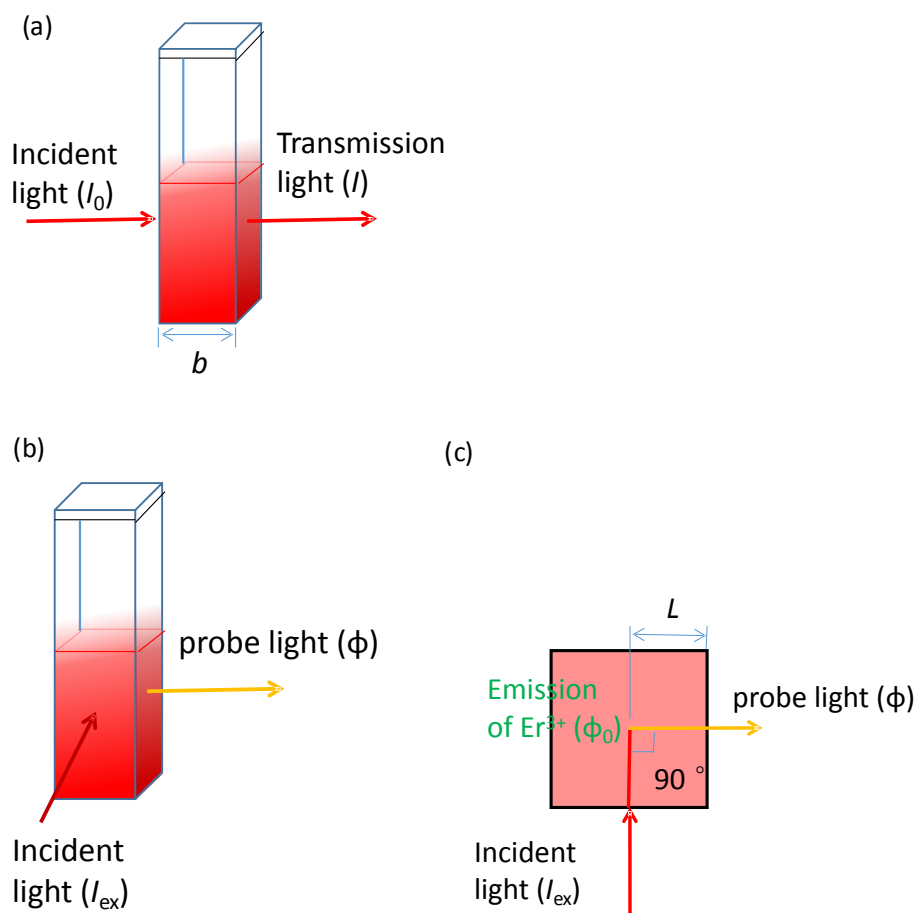


Fig. S8. Optical measurement geometry for (a) absorption, (b, c) excitation and emission spectra: (b) front view, (c) top view.

Absorption cross section(σ) and absorbance(A) are determined by the following equations:

$$\ln\left(\frac{I_0}{I}\right) = \sigma n_1 b \quad (\text{VI})$$

$$n_1 = \frac{N_A c_1}{1000} \quad (\text{VII})$$

$$A = -\lg\left(\frac{I}{I_0}\right) \quad (\text{VIII})$$

Here, n_1 is the number of molecules per cm^3 of the rubrene solution in Fig. S8a, b ($=1 \text{ cm}$) is the

path length of the sample (cm), c_1 is the concentration of the compound (mol/L), N_A is Avogadro's number. We recorded the absorption spectrum of 0.05 mg/mL rubrene and found the absorbance $A=0.36$. According to eq. (VI),(VII) and (VIII), we calculated the absorption cross section of rubrene:

$$\sigma = 1.467 \times 10^{-17} \text{ cm}^2$$

For the process of testing the fluorescence spectrum.

$$\ln\left(\frac{\Phi_0}{\Phi}\right) = \sigma n_2 L \quad (\text{IX})$$

$$n_2 = \frac{N_A c_2}{1000} \quad (\text{X})$$

$$\frac{\Phi_0 - \Phi}{\Phi_0} = 1 - \exp\left(-\frac{\sigma N_A c_2 L}{1000}\right) \quad (\text{XI})$$

where n_2 is the number of molecules per cm^3 of hybrid solution in Fig. S8b, L is the path that the emitted light of Er^{3+} experiences in the sample (cm), c_2 is the concentration of the compound (mol/L), ϕ_0 is the emission intensity of Er^{3+} , ϕ is the emission intensity of the Er^{3+} through the sample.

For $c_2 = 1.41 \times 10^{-3}$ mol/L (0.75 mg/mL), $L=0.5$ cm, according to eq. (XI)

$$\frac{\Phi_0 - \Phi}{\Phi_0} = 99.8\%$$

It means that 99.8% of the visible photons emitted by the upconversion nanoparticles was absorbed when the concentration of rubrene was 0.75 mg/mL. Further, we also estimate the fraction of visible photons reabsorbed by rubrene for a 1-mm thickness sample. The results are shown as follows:

Table S2. The fraction of photons re-absorbed by rubrene for sample thickness of 1 mm.

Sample	Sample 2	Sample 3	Sample 4	Sample 5	Sample 6	Sample 7
C_{RUB} (mg/mL)	0.25	0.50	0.75	1.0	1.5	2.0
$(\Phi_0 - \Phi)/\Phi_0$	33.9%	56.3%	71.1%	80.9%	91.7%	96.4%

Table S3. Derived lifetime values of the hybrid systems

Sample	Sample 1	Sample 2	Sample 3	Sample 4
A_1	-4.586×10^7	-6.446×10^7	-1.367×10^8	1.141×10^9
$A_1/(A_1+A_2)$	1.035	1.023	1.012	0.9987
$\tau_1/\mu\text{s}$	58.83	55.07	49.47	45.43
A_2	1.551×10^6	1.474×10^6	1.526×10^6	1.481×10^6
$A_2/(A_1+A_2)$	-0.035	-0.023	-0.012	0.0013
$\tau_2/\mu\text{s}$	145.3	144.9	141.2	140.5
$\tau_{541\text{ nm}}/\mu\text{s}$	50.95	49.34	46.44	45.81

References

- 1 J. R. Lakowicz, in *Principles of fluorescence Spectroscopy*, 3rd ed. Springer-Verlag: 2008, pp. 99.
- 2 Melika Mahboub , Hadi Maghsoudiganjeh , Andrew Minh Pham , Zhiyuan Huang ,and Ming Lee Tang, Triplet Energy Transfer from PbS(Se) Nanocrystals to Rubrene: the Relationship between the Upconversion Quantum Yield and Size, *Adv. Funct. Mater.* 2016, **26**, 6091 – 6097.
- 3 Zhiyuan Huang, Xin Li, Melika Mahboub, Kerry M. Hanson, Valerie M. Nichols, Hoang Le, Ming L. Tang, and Christopher J. Bardeen, Hybrid Molecule–Nanocrystal Photon Upconversion Across the Visible and Near-Infrared, *Nano Lett.* 2015, **15**, 5552–5557.